

**Purdue University**  
**Purdue e-Pubs**

---

International Compressor Engineering Conference

School of Mechanical Engineering

---

1986

# Heat Transfer in Oil-Flooded Screw Compressors

P. J. Singh

J. L. Bowman

Follow this and additional works at: <https://docs.lib.purdue.edu/icec>

---

Singh, P. J. and Bowman, J. L., "Heat Transfer in Oil-Flooded Screw Compressors" (1986). *International Compressor Engineering Conference*. Paper 521.

<https://docs.lib.purdue.edu/icec/521>

This document has been made available through Purdue e-Pubs, a service of the Purdue University Libraries. Please contact [epubs@purdue.edu](mailto:epubs@purdue.edu) for additional information.

Complete proceedings may be acquired in print and on CD-ROM directly from the Ray W. Herrick Laboratories at <https://engineering.purdue.edu/Herrick/Events/orderlit.html>

## HEAT TRANSFER IN OIL-FLOODED SCREW COMPRESSORS

Pawan J. Singh  
INGERSOLL-RAND COMPANY  
Phillipsburg, N.J.

James L. Bowman  
INGERSOLL-RAND COMPANY  
Mocksville, N.C.

### ABSTRACT

Thermodynamic efficiency of the compression process in oil-flooded screw compressors depends greatly on the oil-gas heat transfer process. The amount of heat transfer is a function of many parameters such as mode of oil injection, oil inlet temperature, etc. This paper describes a mathematical model to calculate this heat transfer, assuming that the oil is injected in the form of non-interacting spherical droplets. The droplet trajectories are calculated from the point of injection to the point where the droplets hit the moving boundaries of the compressor rotor. The overall heat transfer is calculated by summing the heat exchange over all the droplets during their free-flight time. This model is then used to calculate the effect of such heat transfer on compressor performance. Some guidelines on ways to enhance heat transfer are also provided.

## INTRODUCTION

Oil injection in oil-flooded screw compressors serves two primary purposes: one, partial sealing of gas leakage paths, and two, gas cooling through oil-gas heat transfer. The actual extent of heat transfer within the screw compressor cavity is not very well known. Heat transfer estimates obtained from gas discharge temperature measurements include heat transfer both within the cavity and that within the discharge passage up to the measurement point. The latter is normally a large fraction of the total value. In addition, gas temperature measurement in the presence of oil is a very difficult task since the sensor is more likely to measure the temperature of oil than the gas.

It is very important to accurately estimate the amount of heat transfer and find ways to improve it since this is probably the only untapped area in compressor design that can lead to significant improvement in performance. The use of new profiles with smaller leakage contact lines and blow-hole areas, tighter manufacturing clearances and computer programs to optimize design parameters have already resulted in major gains in performance and very little room remains for further large-scale improvements in these areas.

It can be argued that, at least theoretically, changing the compression process from polytropic (typically  $n > 1.4$ ) to isothermal can result in efficiency gains of 15-20%. Yet such gains are not easy to come by for several reasons. Heat transfer in compressor cavities primarily occurs by convection and is a function of the heat transfer coefficient, surface area, temperature difference and time. The heat transfer coefficient is a function of the injection parameters and the temperature difference is a function of operating conditions such as pressure ratio and the location of the injection points. Generally, there is not much latitude for design changes in these areas. The surface area can be increased by several orders by breaking up the oil in very fine droplets (oil-mist injection) as opposed to oil-jet injection. This approach has been tried (1) and shown to yield a few percentage points in efficiency. The oil residence time in the cavity depends on the compressor rpm but is generally of the order of 1-2 msec. For oil-jet injection, time of jet surface area exposure to the temperature difference is even smaller.

Thus it is essential to gain a better understanding of the heat transfer process, particularly with oil-mist injection. In this paper a mathematical model of this process has been developed under certain specified assumptions. This model is then used in a screw compressor performance program (2) to calculate the range of performance improvement for different types of oil injection.

## MATHEMATICAL MODEL

### Assumptions

The model is based on certain assumptions as listed below.

- (i) Oil is injected in the form of spherical droplets of a given size.
- (ii) The oil droplets are non-deformable and non-evaporating.
- (iii) Oil droplet distribution is assumed to be sparse i.e., interaction between droplets is ignored.
- (iv) Heat transfer is calculated only when the droplets are in flight. This is based on observations that droplets tend to agglomerate once they hit a solid boundary, losing their shape and large effective heat transfer surface area.
- (v) The droplets enter a gas flow field that corresponds to rigid body motion of cavities. In other words, the gas in the cavity is carried along with the rotor and the effect of oil droplets on the gas flow field is assumed negligible.

The above assumptions, while being quite restrictive in certain aspects, make it possible to handle an otherwise intractable problem and provide useful guide-lines for maximizing heat transfer and thus improving performance.

### Model Description

Figure 1 shows the oil injection scheme used in the mathematical model. The model equations are based on the polar coordinate system  $(r, \theta, z)$  with origin at the female rotor's center. Oil is sprayed in the female cavity through the housing at point A with initial velocity  $(u_r, u_\theta, u_z)$  in the form of

spherical particles of diameter  $d_p$ . The angular speed of the female rotor is  $\omega$  and the velocity distribution of the gas field within the cavity is given as  $(0, \omega r, U_z)$ . The  $z$  direction is assumed to lie along the rotor axis from inlet port to the discharge port.

The individual droplet trajectories are calculated using Newtonian mechanics and accounting for gas drag forces, centrifugal and coriolis forces. The droplet trajectory ends when the droplet collides with the solid boundaries of the rotor. The droplet is then assumed to stay along the cavity wall and further gas-droplet interaction is terminated from there on.

Since the cavity is rotating, the relative location of the cavity boundary with respect to the droplet keeps shifting. This is illustrated in Figure 2 which shows that the droplet trajectory depends on the droplet location at the point of injection relative to the cavity position. To account for this, the droplets are assumed to be injected at 10 points uniformly along the circumference while the initial cavity position remains the same as shown in Figure 2. Additionally, the cavity boundary conditions are also dependent on the  $z$ -coordinate of the droplet due to the helical nature of the cavity. This is properly accounted for in the model.

Heat transfer is calculated at every integration time step along the trajectory and then used in the calculation of cavity pressure based on first law of thermodynamics. The heat transfer coefficient used in the equations is that for a spherical particle moving in a free gas field. The oil-gas temperature difference depends on the droplet position in the cavity.

It may be pointed out that the model is not restricted to injection in female or male rotor cavities, location of injections points, or injection through the housing or the rotor itself. The mathematical model is easily adaptable to any of these configurations. The only restrictive assumption is that of oil injection in the form of non-interacting spherical droplets. In a sense, this assumption is helpful in that it provides an upper bound on the achievable heat transfer rate.

### Theory

The droplet trajectories are calculated by solving the equations of motion of a particle in a fluid flow field in cylindrical coordinates. These equations, based on Newtonian mechanics, account for the components of the acceleration and drag forces. The gravity force is neglected since it is generally much smaller than the other forces. The equations are based on a fixed cylindrical coordinate system  $(r, \theta, z)$  as shown in Figure 1 and a gas velocity field of  $(0, \omega r, U_z)$ , and are written as

$$\frac{d^2 r}{dt^2} = r \left( \frac{d\theta}{dt} \right)^2 - c_k \frac{dr}{dt} \quad (1)$$

$$r \frac{d^2 \theta}{dt^2} = -2 \frac{dr}{dt} \frac{d\theta}{dt} - c_k \left( r \frac{d\theta}{dt} - U_\theta \right) \quad (2)$$

$$\frac{d^2 z}{dt^2} = -c_k \left( \frac{dz}{dt} - U_z \right) \quad (3)$$

where: 
$$c_k = \frac{18 \mu_g Re C_D}{24 \rho_p d_p^2} \quad (4)$$

$$Re = \frac{\rho_g d_p |U - u|}{\mu_g} \quad (5)$$

And: 
$$C_D = \frac{24}{Re} ; Re \leq 3 \quad (6)$$

$$= \frac{18.5}{Re^{0.6}} ; .3 < Re < 1000 \quad (7)$$

$$= 0.44 ; Re \geq 1000 \quad (8)$$

$C_D$  is the drag coefficient for a spherical particle moving in a gas field at a relative Reynolds number  $Re$  while  $C_K$  represents the drag force/unit velocity. The first term on the right hand side of equations (1) and (2) represent centrifugal and coriolis accelerations respectively.

The gas velocity field  $U$  is defined by,

$$U_r = 0 \quad (9)$$

$$U_\theta = \omega r \quad (10)$$

$$U_z = \frac{\omega L}{\alpha} \quad (11)$$

The initial conditions are given as follows:

$$r(0) = R, \quad \theta(0) = 0, \quad z(0) = 0 \quad (12)$$

$$\frac{dr}{dt}(0) = U_{ri}; \quad \frac{d\theta}{dt}(0) = \frac{U_\theta}{R}; \quad \frac{dz}{dt}(0) = U_{zi} \quad (13)$$

$U_{ri}$ ,  $U_{\theta i}$ ,  $U_{zi}$  are the droplet velocity components at the point of injection, i.e.,  $\Delta t = 0$ . Equations (1) to (11) along with initial conditions (12) and (13) are integrated in time at equal time steps of size  $\Delta t$  using Euler's method. The integration is terminated when the particle hits the cavity boundary.

The heat transfer rate  $H_p$  for one droplet is given by,

$$H_p = h A_p \Delta T \quad (14)$$

where

$$A_p = \frac{\pi d_p^2}{4} \quad \Delta T = T_g - T_p \quad (15)$$

The heat transfer coefficient  $h$  for a spherical particle in a free gas field has been experimentally determined (3) as:

$$\frac{h d_p}{k_g} = 2.0 + 0.6 Re^{0.5} Pr^{0.33} \quad (16)$$

The total heat transfer rate for all droplets is calculated by summing individual heat transfer rates for ten distributed droplets and then averaging it over all droplets per unit time N,

$$H = \sum_{i=1}^{10} H_{Pi} \frac{N}{10} \quad (17)$$

where

$$N = \frac{m_{oil}}{\rho_p (\pi d_p^3 / 6)} \quad (18)$$

This value of H is used during the droplet flight time to calculate cavity pressure  $P_c$  and compressor performance according to the following relationship as given in reference 2:

$$\frac{dP_c}{dt} = \frac{\gamma - 1}{V_c} H - \frac{\gamma P_c}{V_c} \frac{dV_c}{dt} - \frac{\gamma P_c}{\rho_g V_c} \dot{m}_{L_{out}} + \frac{\gamma}{V_c} \sum \frac{P_{in}}{\rho_{gin}} \dot{m}_{Lin} \quad (19)$$

#### Droplet Size

Small droplets can be produced by atomization of the oil injection stream. When oil is injected in a gas stream, it is broken up by aerodynamic forces due to relative motion between the phases. The most effective way to break liquid into droplets is to create a thin sheet of liquid and then break it with single or multiple gas jets. The appendix describes a method of calculating final droplet size when a large drop is introduced into a gas stream at high values of the Weber number W,

$$W = \frac{\rho_g |U - u| d_p}{\sigma_p}$$



The relative velocity  $|U-u|$  is a function of the initial injection velocity which further depends on the injection pressure. In most screw compressor applications, the oil injection process is driven by the difference in discharge pressure and cavity pressure at the time of injection. This limits the droplet size unless external means are used to break up the jet before injection. Positive-displacement oil pumps are frequently used to boost the oil injection pressure which can result in smaller droplets but the power savings from additional heat transfer must be balanced against the oil pump power. Figure 3 shows plots of injection velocity through a .032" orifice and droplet size (based on equation 20) as a function of pressure difference.

## RESULTS

As mentioned earlier, in the results presented here the droplets have been assumed to be injected radially at ten uniformly spaced locations on the circumference. For cases where the oil is injected through a series of small holes scattered over a certain area, the model can be applied by calculating trajectories starting at several different axial locations.

In the results described, the droplets are also assumed to be of the same diameter in order to isolate the effects of size and enable parametric studies to be performed. In practice, however, the droplets are of varying size. This can be easily accounted for in the model by assuming a statistical distribution of droplet sizes with a certain mean diameter and standard deviation (e.g. the Sauter mean diameter).

Figures 4 to 6 show the droplet trajectories in the x-y plane for 10, 100, and 1000  $\mu$ m diameter droplets, respectively. The droplets in each case are injected radially at 20m/sec at ten locations around the circumference. The position of the injection points are numbered 1 through 10, with position 1 located on the ordinate. The rotor tip speed for these plots is 30m/sec. The dotted profile shape is the rotor position at zero time when the trajectory calculation starts.

From these figures, it is clear that while the smaller 10 or 100  $\mu$ m droplets have a tendency of centrifuging out after being slowed by the drag forces,

the larger  $1000\text{ }\mu\text{m}$  droplets travel virtually in a straight line. This is because the inertial forces vastly outweigh the drag forces for the large droplets. In all these figures, various droplets have different trajectories depending on the droplet's initial position relative to the profile. Droplets from position nos. 5 to 10 generally have short trajectories because they hit the profile before reaching the maximum lobe depth. In fact, only a few droplets have the freedom to complete their trajectories unaffected by the rotor.

Figure 7 shows  $1000\text{ }\mu\text{m}$  droplet trajectories in the x-y plane for initial injection velocities of 20, 40 and 60 m/sec. In each case, the droplets are rapidly decelerated by the gas drag and then centrifuged out (unless they hit the rotor boundary). The only difference is that at higher injection velocities, droplets travel farther inwards before centrifugal forces become dominant. But the total time of free flight during which the most effective heat transfer takes place is actually less for the higher velocity droplets although the heat transfer coefficient is larger due to increased relative velocity. The method used here accounts for all these factors in determining the effective heat transfer and its effect on performance. Figure 8 shows the radial, tangential and axial velocity components for  $1000\text{ }\mu\text{m}$  droplets injected at an initial radial velocity of 20 m/sec from position No. 3. The radial velocity sharply decreases with time due to the drag forces while the axial and tangential velocities increase as the droplet is dragged along by the rotating gas field. The total time of free flight is only 1.33 msec which for this particular case translates into 29 degrees of rotation.

Table 1 shows the normalized specific power, volumetric efficiency (VE), bulk discharge gas temperature and oil temperature for three cases. Case 1 is the standard orifice injection technique while in cases 2 and 3, oil is injected in the form of droplets of 100 and  $1000\text{ }\mu\text{m}$  diameter respectively. The BHP is normalized to the standard case (Case 1) BHP. For all cases, oil is injected into a closed cavity at  $\theta_c = 540^\circ$  (or a pressure ratio of about 3) and the inlet gas and oil temperature are  $80^\circ$  and  $130^\circ\text{F}$ , respectively. The results indicate performance improvement of 7.0% for  $1000\text{ }\mu\text{m}$  particles and 8.3% for  $100\text{ }\mu\text{m}$  particles. The VE and the capacity are essentially unchanged. The bulk discharge gas

temperature decreases substantially with droplet injection due to much improved heat transfer while the discharge oil temperature rises, in comparison to the standard jet injection case.

Figure 9 shows the effect of varying the injection point location from  $400^\circ$  to  $590^\circ$  on specific power and bulk discharge gas temperature for  $100\text{ }\mu\text{m}$  particles. Note that the inlet port closes at  $372^\circ$  and the discharge port opens at  $604^\circ$ . An optimum injection point ( $540^\circ$ ) is clearly identified corresponding to minimum specific power and maximum compressor efficiency. The U-shaped performance curve can be explained as follows: At  $400^\circ$  oil injection, the compression process has just begun. The gas and oil temperatures are not far apart and the heat transfer is low. At  $490^\circ$  oil injection, the cavity pressure and gas temperature are higher and the heat transfer is increased. The amount of heat transfer increases with increasing injection angle until  $540^\circ$ . Beyond this the heat transfer reduces because most of the compression has already occurred and part of the injection actually takes place following opening of the discharge port. Thus, the heat transfer process is most effective in cooling the air and less useful in improving compression efficiency.

#### DISCUSSION OF RESULTS

The method outlined in this paper presents an idealized albeit useful model for calculating the amount of heat transfer and its effect on the performance of oil-flooded screw compressors. The method can also be used in optimizing the oil injection quantity, location and direction of injection ports, injection velocity, and droplet size. It is clear that increasing the available surface area by atomizing the oil into small droplets has a significant effect on performance. For example, the results indicate that atomizing oil into  $1000\text{ }\mu\text{m}$  (.04 in) droplets can result in HP savings of about 7%. Even if only half of these savings could be realized in practice, it is still significant. These predictions are in general agreement with some limited test data available to the authors.

The results also indicate that while  $100\text{ }\mu\text{m}$  droplets improve performance further, the gain is not substantial. Smaller droplets require higher injection velocities which further require high pressure differentials across the injection holes. If the

droplets could be held to a reasonable size, supplementary means of boosting oil pressure such as an oil pump may not be necessary. In addition, the results show that location of the oil injection point is just as important as the oil droplet size. Injection into the cavity during early stages of compression is not useful since the temperature difference during the heat transfer is very low. It is not productive to inject very late either because most of the compression power has already been consumed by then. The model offered here can be used to find optimum injection location as well as injection pattern.

It must not be overlooked that oil injection serves another very important function of partially sealing rotor tip leakage. The needs for effective sealing and good heat transfer can be effectively combined to yield the best performing compressor design. For example, a small quantity of oil could be uniformly distributed over most of the compression cavity for effective sealing while the rest of the oil could be injected at selected locations for optimum heat transfer.

### CONCLUSIONS

A method to compute oil-gas heat transfer in oil-flooded screw compressors and its effect on compressor performance has been presented. According to this method, oil is injected in the form of spherical droplets of small size at specified locations. The results show that this type of injection can lead to significant gains in performance. The level of performance improvement is dependent on several design parameters such as location and size of injection holes, oil temperature, etc. Some guidelines for selection of these parameters have been presented. The optimum combination of these parameters can be determined by using the method presented here.

### ACKNOWLEDGEMENTS

The authors are thankful to Ingersoll-Rand management for permission to publish this paper.

## SYMBOLS

A	=	Area
$C_D$	=	Drag coefficient
$C_p$	=	Specific heat at constant pressure
d	=	Diameter
h	=	Heat transfer coefficient
H	=	Heat transfer rate
k	=	Gas thermal conductivity
L	=	Rotor length
$m_{oil}$	=	Oil mass injected/unit time
$m_L$	=	Leakage mass flow rate
N	=	No. of droplets/unit time
Pr	=	Gas Prandtl no. = $(\mu C_p/k)$
r, $\theta$ , z	=	radial, circumferential and axial coordinates
R	=	Rotor radius
Re	=	Reynolds number
t	=	Time
T	=	Temperature
V	=	Cavity volume
W	=	Weber number
d/dt	=	Time derivative
$\alpha$	=	Wrap angle in radius
$\gamma$	=	Specific heat ratio
$\eta$	=	Molecular viscosity
$\omega$	=	Angular velocity
$\rho$	=	Density
$\sigma$	=	Surface tension

## SUBSCRIPTS

c	=	Cavity
g	=	Gas
i	=	Initial condition
in	=	Inlet leakage flow
L	=	Leakage flow
out	=	Out of cavity leakage flow
p	=	droplet

## REFERENCES

1. U. S. Patent No. 3820923, 1974
2. Singh, P. J., and Patel, G. C., "A Generalized Performance Computer Program for Oil Flooded Twin-SCrew Compressors", 1984 International Compressure Engineering Conference Proceedings, Purdue
3. Ranz W., and Marshall, W., Jr., "Evaporation from Drops," Chemical Engineering Progress, Vol. 48, 1952
4. Masugi Isshiki, N: Rept. 35, Transportation Technical Research Institute, Tokyo, Japan, July, 1959

## APPENDIX

When a liquid jet stream is injected in a gas stream at high velocities, a large number of small liquid drops are formed by shattering of the continuous jet. The most important dimensionless group for determining the stability and breakup of a droplet as mentioned in the text of the paper is the Weber Number W.

For a drop introduced into a gas stream at high values of W, an expression for the final drop size following successive breakups is given by (Isshiki (4)),

$$\left(\frac{d}{d_o}\right)^{0.25} = \frac{1.9}{W_o^{0.25}} + .315 \left(\frac{\rho_g}{\rho_f}\right)^{1.5} C_{D_o} W_o^{0.125} \ln\left(\frac{d}{d_o}\right)$$

Where subscript o refers to the initial conditions which can be assumed to be those at the orifice, i.e.  $d_o$  = orifice diameter.  $C_{D_o}$  is the drag coefficient which can be taken as 1.

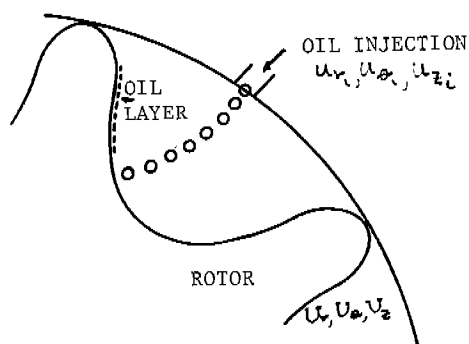


Figure 1 - Rotor and Oil Injection Schematic.

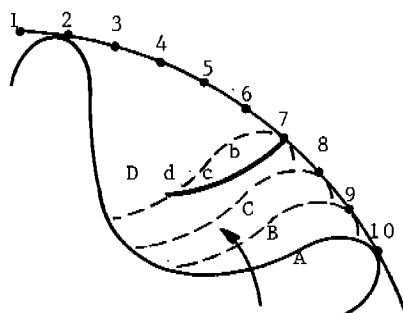


Figure 2 - Location of 10 Injection Points Located Along The Circumference. Dotted Lines Show Rotor Positions at Three Instants. Points b, c, d, Represent Trajectory of Particle 7 at Three Instants Before Hitting Rotor at d.

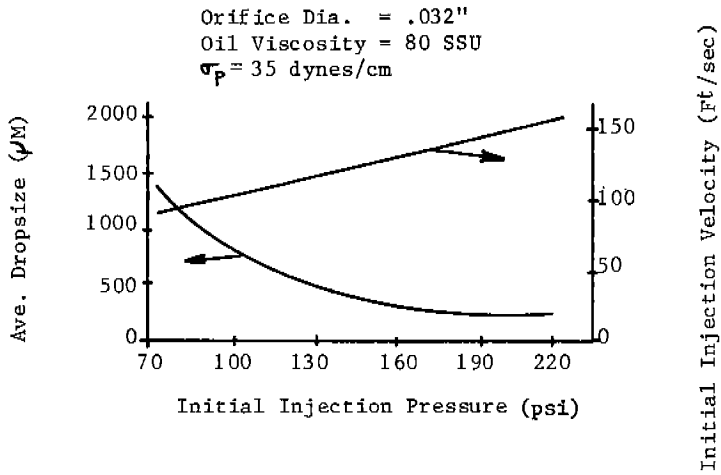


Figure 3 - Injection Velocity and Oil Droplet Size As a Function of Injection Pressure.

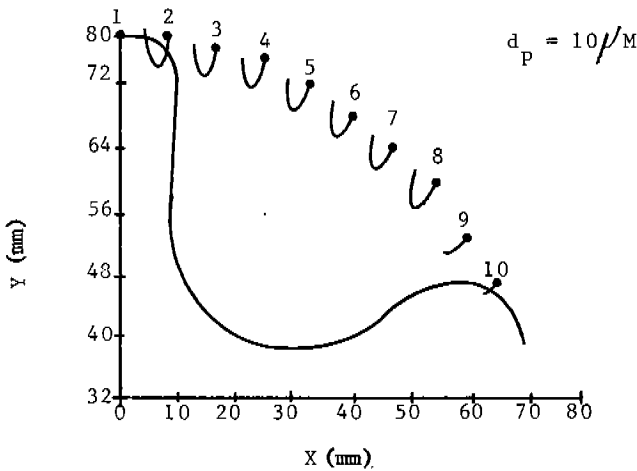


Figure 4 - Droplet Trajectories for  $10 \mu\text{M}$  Droplets.  
Injection Velocity = 20 m/sec.  
Rotor Profile Is Shown At Initial Position.



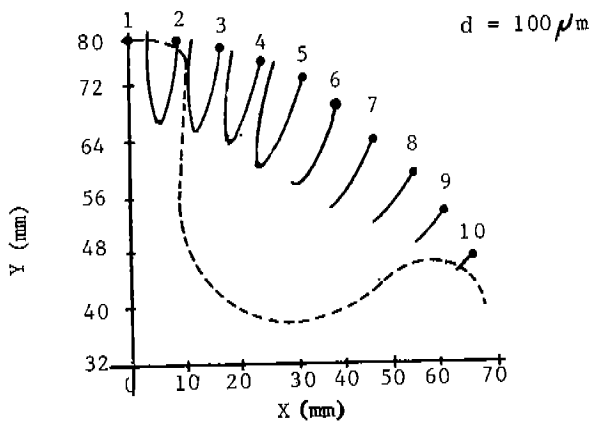


Figure 5 - Droplet Trajectories for 100  $\mu\text{m}$  Droplets.  
Injection Velocity = 20 m/sec.

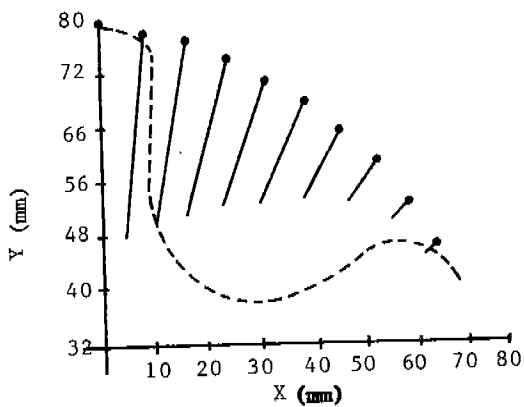


Figure 6 - Droplet Trajectories for 1000  $\mu\text{m}$  Droplets.  
Injection Velocity = 20 m/sec.

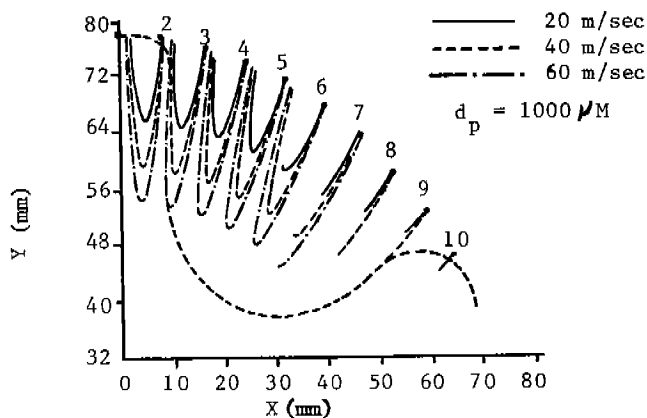


Figure 7 - Droplet Trajectories for  $1000 \mu\text{M}$  Droplets With Varying Injection Velocities.

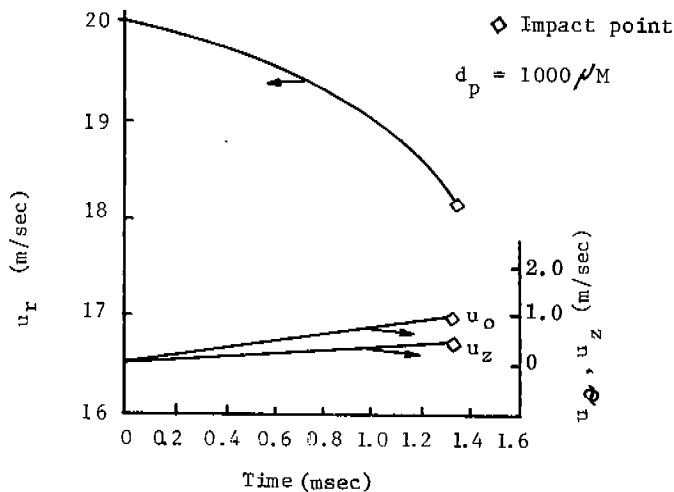


Figure 8 - Radial, Axial, and Tangential Velocities for  $1000 \mu\text{M}$  Droplet. Initial Radial Injection Velocity =  $20 \text{ m/sec}$ .

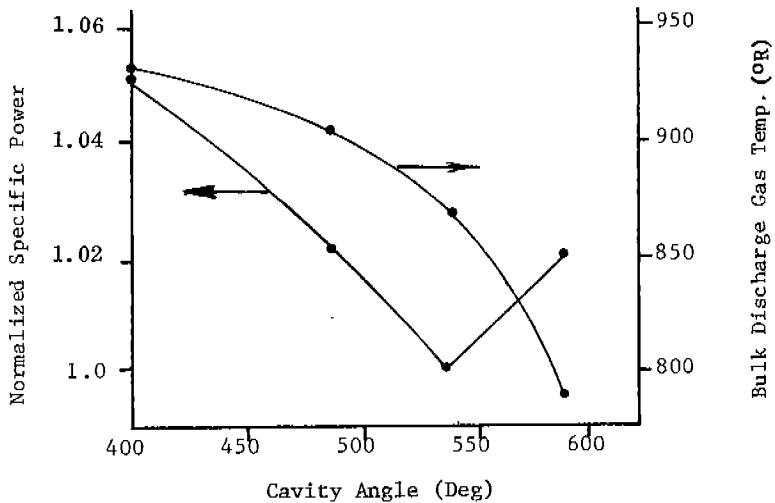


Figure 9 - Normalized Specific Power and Bulk Discharge Gas Temperature As A Function of Injection Location.

TABLE 1

Case No.	Droplet Dia. (μM)	Normalized Specific Power	V.E. (%)	Bulk Discharge Temp. °F	
				Gas * (°F)	Oil ** (°F)
1	Standard (Jet Injection)	1.0	87.6	507.6	146.5
2	1000	0.930	87.9	406.1	154.6
3	100	0.917	88.0	393.6	155.1
* - Inlet Gas Temperature = 80°F ** - Inlet Oil Temperature = 130°F					

## THE INTERCOOLER WITH SPRAYING WATER FOR AIR COMPRESSORS

Kang Yong

Division of Air Conditioning, Department of Textile Engineering, North-west Institute of Textile Science and Technology, Xi'an, China

### ABSTRACT

A spraying water device to cool gas can be used in the intercooler of air compressors instead of the heat exchanger. It is more effective for heat transfer because the gas is in direct contact with the cooling water sprayed on to the gas. This paper gives the cooling form, the separating water method from gas, and the calculating formula for heat transfer. Through experiments under the normal pressure, the calculated result of the formula is satisfactory and the separating process, using a group of streamline baffles to block water, has a low pressure drop and a better separating effect, water content is 0.1 % after separation. The content does not influence the next compression.

### SYMBOLS

F	resistance
C	resistance coefficient
R	density
L	average diameter of drops
V	velocity
t	time
a	acceleration
m	drop mass
Re	Reynolds number
Z	length
v	viscous-force
B	distance between the baffles